

See discussions, stats, and author profiles for this publication at: <https://www.researchgate.net/publication/6935286>

# Electron Paramagnetic Resonance Study of Partially Oriented Clay Platelets Intercalated with Copper(II) 1,4,8,11-Tetraazacyclotetradecane

ARTICLE *in* THE JOURNAL OF PHYSICAL CHEMISTRY B · APRIL 2005

Impact Factor: 3.3 · DOI: 10.1021/jp0454826 · Source: PubMed

---

CITATIONS

9

---

READS

26

4 AUTHORS, INCLUDING:



Hyun Jung

Dongguk University

54 PUBLICATIONS 669 CITATIONS

SEE PROFILE



Jin-Ho Choy

Ewha Womans University

478 PUBLICATIONS 9,817 CITATIONS

SEE PROFILE

# Electron Paramagnetic Resonance Study of Partially Oriented Clay Platelets Intercalated with Copper(II) 1,4,8,11-Tetraazacyclotetradecane

Hyunsoo So,<sup>\*,†</sup> Hyun Jung,<sup>‡</sup> Jin-Ho Choy,<sup>‡</sup> and R. Linn Belford<sup>§</sup>

Department of Chemistry, Sogang University, Seoul 121-742, Korea, Division of Nanoscience and Department of Chemistry, Ewha Womans University, Seoul 120-750, Korea, and Illinois EPR Research Center and Department of Chemistry, University of Illinois at Urbana-Champaign, Illinois 61801

Received: October 5, 2004; In Final Form: December 21, 2004

Electron paramagnetic resonance (EPR) spectra of powder and oriented films of montmorillonite, hectorite, and saponite intercalated with  $[\text{Cu}(\text{cyclam})]^{2+}$  (cyclam = 1,4,8,11-tetraazacyclotetradecane) exhibit three components: an orientation-dependent component without hyperfine features, an orientation-dependent component with hyperfine features, and an orientation-independent component without hyperfine feature. EPR spectra of  $[\text{Cu}(\text{cyclam})]^{2+}$ -saponite, which exhibit only two components and the best resolved hyperfine features, were simulated. The spectra indicate that a large portion of the saponite platelets are inclined to the glass surface, although they tend to align with their basal planes parallel to the glass surface. The orientation-dependent spectra could be simulated by introducing a Gaussian distribution with a standard deviation of  $20^\circ$  for the inclination angle. The standard deviation may be used as a disorder parameter for the microcrystals assembled on glass plates. Spectral simulation also shows that the  $\text{CuN}_4$  plane of  $[\text{Cu}(\text{cyclam})]^{2+}$  is parallel to the clay layers. EPR spectra of some other partially oriented systems are also discussed.

## Introduction

Single-crystal electron paramagnetic resonance (EPR) spectra can provide information on the orientation of paramagnetic species in a crystal. This information, which is vital in characterizing the paramagnetic species for many important systems, is lost for powder samples. Yet many EPR studies have been carried out with powder samples, for it is difficult to grow large crystals suitable for single-crystal EPR studies. We have been interested in extracting information on molecular orientation from EPR spectra of partially oriented systems. Recently some of us observed single-crystal-type EPR spectra from monolayers of copper-exchanged zeolite Na-A microcrystals assembled on glass plates and obtained information on the orientations of the copper species.<sup>1</sup> The monolayers consisted of small domains in which microcrystals were oriented in the same direction, but the domains were randomly oriented on the glass surface. So, although it was a partially oriented system, it produced a single-crystal-type spectrum when the magnetic field was perpendicular to the glass surface.

For this work, we have chosen intercalated clays assembled on glass plates, which are partially oriented systems with much larger disorder. Since clay platelets tend to assemble on glass plates with their basal planes parallel to the glass surface, clay films were used to study anisotropic properties of the intercalated molecules. Some EPR studies have been carried out on oriented clay films to determine orientations of the intercalated molecules.<sup>2–5</sup> However, EPR spectra for these partially oriented systems have not been fully explored.

Recently some of us used oriented clay films to study polarization-dependent X-ray absorption spectra of  $[\text{Cu}(\text{cy-}$

$\text{clam})]^{2+}$  intercalated in saponite.<sup>6</sup> The peak assignments from the polarization experiment were then used to assign the peaks in the X-ray absorption near-edge structure spectra of the powder sample. The saponite platelets were assumed to be partially oriented on the glass surface, but it has never been determined how orderly these assemblies are.

In this work, we report EPR studies of oriented films of montmorillonite, hectorite, and saponite intercalated with  $[\text{Cu}(\text{cyclam})]^{2+}$ . The molecular structure of  $[\text{Cu}(\text{cyclam})]^{2+}$  was reported before (Figure 1).<sup>7,8</sup> The four nitrogen atoms in the macrocyclic ligand form a square planar arrangement around the copper ion. Frozen solution EPR spectra of pure  $[\text{Cu}(\text{cyclam})]^{2+}$  were reported previously,<sup>8–10</sup> and they could be simulated using an axial spin Hamiltonian. The powder XRD patterns for montmorillonite, hectorite, and saponite intercalated with  $[\text{Cu}(\text{cyclam})]^{2+}$  were given elsewhere.<sup>6,11,12</sup> The spacing of the interlayers (or gallery spacing) is 3.75–3.86 Å, indicating that  $[\text{Cu}(\text{cyclam})]^{2+}$  is intercalated as a monolayer with the square plane of  $\text{CuN}_4$  roughly parallel to the clay layers.

EPR spectra of  $[\text{Cu}(\text{cyclam})]^{2+}$  intercalated in montmorillonite, hectorite, and saponite reveal three components. Since the hyperfine lines of copper species are most sensitive to the molecular orientation, we have chosen  $[\text{Cu}(\text{cyclam})]^{2+}$ -saponite, showing only two components and the best resolved hyperfine features, to simulate EPR spectra of the oriented films. To simulate the orientation-dependent spectra, we have introduced a Gaussian distribution for the inclination angle of the saponite platelets to the glass surface. The resulting standard deviation of this Gaussian distribution may be used as a disorder parameter measuring how disorderly the clay platelets are as assembled on the glass surface.

## Experimental Section

**Materials.**  $[\text{Cu}(\text{cyclam})](\text{ClO}_4)_2$  was prepared as previously reported.<sup>11</sup> For the syntheses of  $[\text{Cu}(\text{cyclam})]^{2+}$ -saponite

\* To whom correspondence may be addressed. E-mail: hyunso@sogang.ac.kr.

<sup>†</sup> Sogang University.

<sup>‡</sup> Ewha Womans University.

<sup>§</sup> University of Illinois.

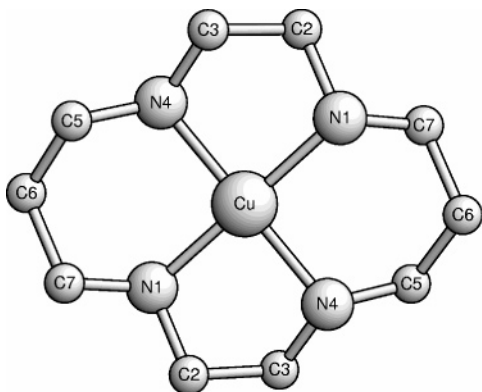


**Figure 1.** Schematic representation of  $[\text{Cu}(\text{cyclam})]^{2+}$  ion.

intercalation compound at high cation-exchange capacity (CEC) loading,<sup>6</sup> 0.5 g of saponite (Sumecton SA purchased from Kunimine Ind. Co.) was immersed in an aqueous solution of  $[\text{Cu}(\text{cyclam})](\text{ClO}_4)_2$  (0.5 g/50 mL) at 60 °C for a week. The exchanged clay was centrifuged and washed several times with deionized water. The wet  $[\text{Cu}(\text{cyclam})]^{2+}$ -saponite compound thus obtained was dispersed in distilled water and then cast or spin-coated onto  $18 \times 18 \text{ mm}^2$  thin glass plates. Finally, the film and the wet powder were freeze-dried in a vacuum ( $<10^{-5}$  Torr). For the synthesis of a sample at low CEC loading, an aqueous solution of  $[\text{Cu}(\text{cyclam})](\text{ClO}_4)_2$  (0.05 g/50 mL) was used.  $[\text{Cu}(\text{cyclam})]^{2+}$ -montmorillonite and -hectorite were prepared in a similar way.<sup>11,12</sup> The compositions of prepared samples determined using ICP analysis are as follows:

$[\text{Cu}(\text{cyclam})]^{2+}$ -montmorillonite,  $\text{Na}_{0.06}[\text{Cu}(\text{cyclam})]_{0.36}(\text{Al}_{3.20}\text{Mg}_{0.64}\text{Fe}_{0.16})(\text{Si}_{7.78}\text{Al}_{0.22})\text{O}_{20}(\text{OH})_4$ ;

$[\text{Cu}(\text{cyclam})]^{2+}$ -hectorite,  $\text{Na}_{0.20}[\text{Cu}(\text{cyclam})]_{0.30}(\text{Mg}_{5.30}\text{Li}_{0.70})(\text{Si}_{7.90}\text{Al}_{0.10})\text{O}_{20}(\text{OH})_4$ ;

$[\text{Cu}(\text{cyclam})]^{2+}$ -saponite,  $\text{Na}_{0.16}[\text{Cu}(\text{cyclam})]_{0.28}(\text{Mg}_{5.98}\text{Al}_{0.02})(\text{Si}_{7.26}\text{Al}_{0.74})\text{O}_{20}(\text{OH})_4$ ;

low-loading  $[\text{Cu}(\text{cyclam})]^{2+}$ -saponite,  $\text{Na}_{0.56}[\text{Cu}(\text{cyclam})]_{0.08}(\text{Mg}_{5.98}\text{Al}_{0.02})(\text{Si}_{7.26}\text{Al}_{0.74})\text{O}_{20}(\text{OH})_4$ .

**Measurements.** EPR measurements were performed on a Varian E-122 X-band spectrometer (12 in. magnet). The microwave frequency was determined with an EIP frequency meter, and powdered DPPH was used as a  $g$  marker. EPR spectra of powder samples and the clay films prepared on glass plates were measured at room temperature and at 77 K. Five thin glass plates ( $3 \times 18 \text{ mm}^2$ ) were stacked up and attached to a quartz rod in a goniometer, and EPR signals were accumulated about ten times. Since spin-coated glass plates exhibited very weak EPR signals, all measurements were performed using samples prepared by casting.

## Results

**Powder Spectra.** Powder EPR spectra of  $[\text{Cu}(\text{cyclam})]^{2+}$ -montmorillonite, -hectorite, and -saponite measured at 77 K are shown in Figure 2.  $[\text{Cu}(\text{cyclam})]^{2+}$ -montmorillonite shows an anisotropic spectrum having no hyperfine feature. The spectra of  $[\text{Cu}(\text{cyclam})]^{2+}$ -hectorite and  $[\text{Cu}(\text{cyclam})]^{2+}$ -saponite consist of two components each, the major component (component A) having no hyperfine feature and the minor component (component B) exhibiting some hyperfine features.

The spectra were simulated with second-order perturbation equations for an axial system. The effect of two isotopes of copper,  $^{63}\text{Cu}$  (69.2%,  $I = 3/2$ ) and  $^{65}\text{Cu}$  (30.8%,  $I = 3/2$ ) was included explicitly in the simulation. The spectrum for  $[\text{Cu}(\text{cyclam})]^{2+}$ -montmorillonite and component A for  $[\text{Cu}(\text{cyclam})]^{2+}$ -hectorite and -saponite were simulated with a

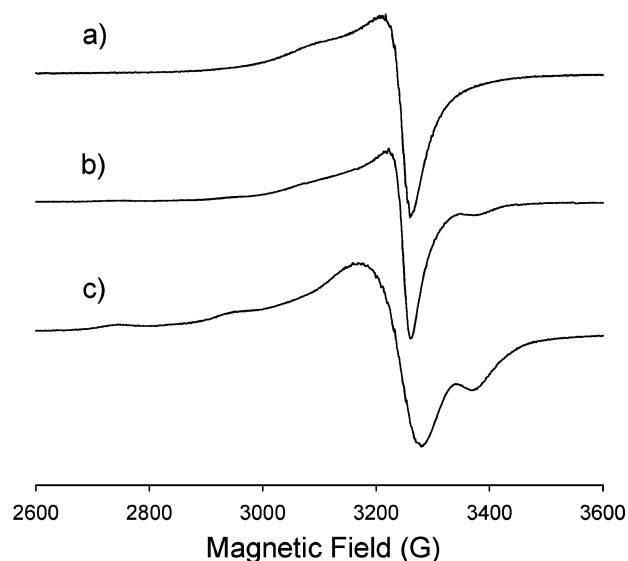


**Figure 2.** Powder EPR spectra of  $[\text{Cu}(\text{cyclam})]^{2+}$  intercalated in (a) montmorillonite, (b) hectorite, and (c) saponite measured at 77 K.

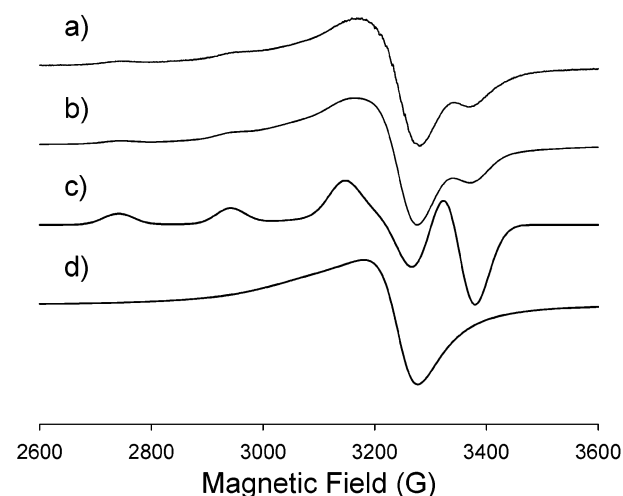


**Figure 3.** (a) Experimental and (b) simulated powder EPR spectra of  $[\text{Cu}(\text{cyclam})]^{2+}$ -saponite measured at 77 K. (c) Component B. (d) Component A.

Lorentzian line shape. At this stage, the line shape for component B was not clear, for this component was relatively weak, and the lines were broad. But the spectra for the oriented film of  $[\text{Cu}(\text{cyclam})]^{2+}$ -saponite clearly show that the line shape of component B is close to the Gaussian line shape (see below). The line width  $w$  was calculated by

$$w^2 = w_{\parallel}^2 \cos^2 \theta + w_{\perp}^2 \sin^2 \theta$$

where  $\theta$  is the angle between the magnetic field and the  $g_{\parallel}$  direction.<sup>13</sup> Experimental and simulated spectra for  $[\text{Cu}(\text{cyclam})]^{2+}$ -saponite and separate spectra for components A and B are shown in Figure 3. Table 1 gives the resulting EPR parameters, half line widths, and the intensity ratio of the two components.

**Oriented Films.** To simulate the spectra of oriented films, some axes are defined in Figure 4. The axis normal to the glass surface is defined as the  $z$  axis, and the  $x$  and  $y$  axes are two orthogonal axes arbitrarily chosen in the glass surface. The angle between the magnetic field ( $B$ ) and the  $z$  axis is denoted by  $\alpha$ . EPR spectra were measured for every  $5^\circ$  for the magnetic field in the  $xz$  plane. The spectra measured at room temperature and at 77 K were essentially the same.

**TABLE 1: EPR Parameters of [Cu(cyclam)]<sup>2+</sup> in Different Clays**

	montmorillonite powder <sup>a</sup>	hectorite powder <sup>a</sup>	saponite powder <sup>a</sup>	saponite film <sup>b</sup>
Component A				
$g_{  }$	2.151	2.151	2.160	2.160
$g_{\perp}$	2.041	2.040	2.040	2.043
$w_{  }/G$	80	80	150	150
$w_{\perp}/G$	32	25	60	38
Component B				
$g_{  }$		2.176	2.179	2.173
$g_{\perp}$		2.046	2.046	2.038
$A_{  }/\text{cm}^{-1}$		0.0200	0.0200	0.0200
$A_{\perp}/\text{cm}^{-1}$		0.0029 <sup>c</sup>	0.0029 <sup>c</sup>	0.0029 <sup>c</sup>
$w_{  }/G$		40	30	30
$w_{\perp}/G$		35	40	30
intensity ratio (A/B)			6.5	6.5

<sup>a</sup> Measured at 77 K. <sup>b</sup> Measured at room temperature. <sup>c</sup> Taken from ref 10.

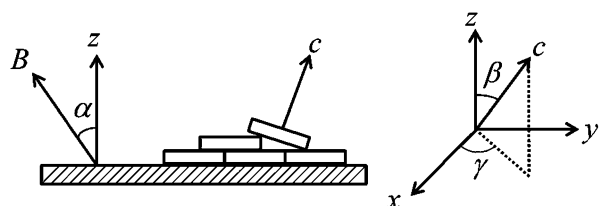


**Figure 4.** Definition of axes and angles. The  $z$  axis is normal to the glass surface, and the  $x$  and  $y$  axes are orthogonal axes arbitrarily chosen in the glass surface. The  $c$  axis is normal to the basal plane of a clay platelet. The direction of the  $c$  axis is defined by the polar angle,  $\beta$ , and the azimuthal angle,  $\gamma$ . The angle between the magnetic field ( $B$ ) and the  $z$  axis is denoted by  $\alpha$ .

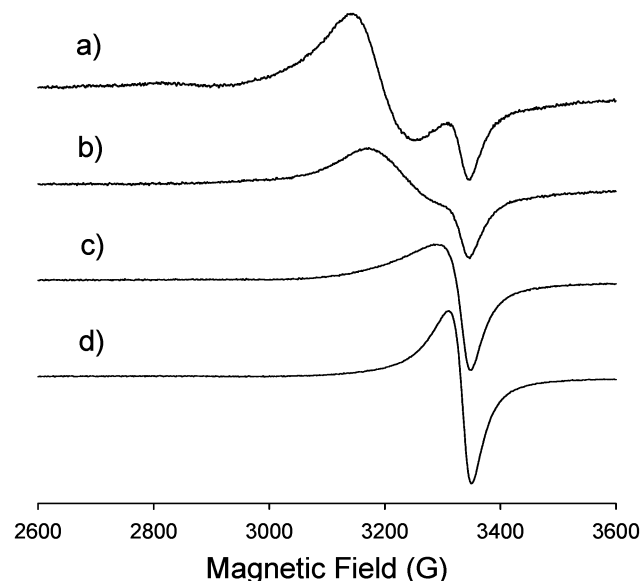


**Figure 5.** EPR spectra of [Cu(cyclam)]<sup>2+</sup>—montmorillonite in oriented films for (a)  $\alpha = 0^\circ$ , (b)  $\alpha = 30^\circ$ , (c)  $\alpha = 60^\circ$ , and (d)  $\alpha = 90^\circ$ . The spectra were measured at room temperature.

Some EPR spectra of [Cu(cyclam)]<sup>2+</sup>—montmorillonite are shown in Figure 5. The spectra consist of a broad, orientation-dependent component that agrees with the powder spectrum and an additional isotropic component (component C). Component C is not seen in the powder spectrum, probably hidden under the perpendicular portion. EPR spectra of [Cu(cyclam)]<sup>2+</sup>—hectorite consist of components A, B, and C (Figure 6). Again component C is not seen in the powder spectrum.

We have chosen [Cu(cyclam)]<sup>2+</sup>—saponite, showing only two components and the best resolved hyperfine features, to simulate EPR spectra of oriented films. As shown in Figure 7, the EPR spectrum is sensitive to the orientation of the magnetic field,

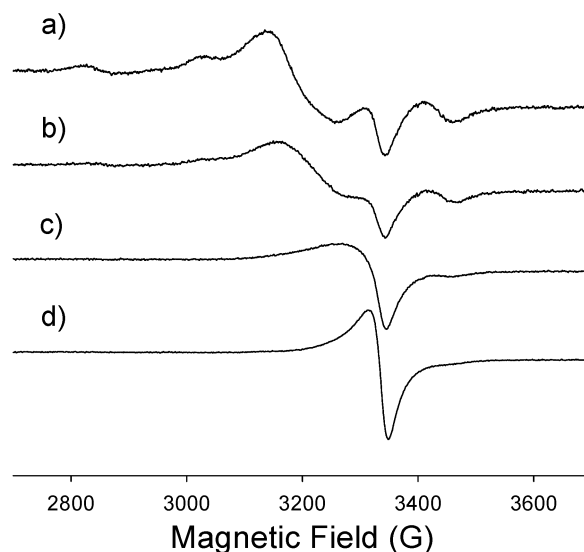


**Figure 6.** EPR spectra of [Cu(cyclam)]<sup>2+</sup>—hectorite in oriented films for (a)  $\alpha = 0^\circ$ , (b)  $\alpha = 30^\circ$ , (c)  $\alpha = 60^\circ$ , and (d)  $\alpha = 90^\circ$ . The spectra were measured at room temperature.

but the angular dependence is not like that of a single-crystal spectrum. When the magnetic field is parallel to the  $z$  axis, the spectrum exhibits a broad featureless line of component A and four hyperfine features of component B. The  $g_{||}$  and  $A_{||}$  values of component B suggest that the  $g_{||}$  direction tends to align parallel to the  $z$  axis. If the  $g_{||}$  directions of all intercalated molecules were parallel to the  $z$  axis, the hyperfine lines should move upfield when the magnetic field moves away from the  $z$  axis. But positions of the hyperfine features do not change even at  $\alpha = 30^\circ$ ; only their relative intensity decreases, indicating that there are some molecules having the  $g_{||}$  direction parallel to the magnetic field even at  $\alpha = 30^\circ$ .

Since the gallery spacing for [Cu(cyclam)]<sup>2+</sup>—saponite is only 3.75 Å,<sup>6</sup> it is reasonable to assume that the orientation of [Cu(cyclam)]<sup>2+</sup> in the gallery of saponite is fixed. Then, the characteristic hyperfine features should be attributed to the clay platelets inclined to the glass surface. Let us define the axis normal to the basal plane of a clay platelet as the  $c$  axis, and the direction of the  $c$  axis on the glass surface by the polar angle,  $\beta$ , and the azimuthal angle,  $\gamma$  (Figure 4). If a Gaussian distribution is introduced for the  $c$  axis, then the number of clay platelets at the angle  $\beta$  for a given azimuthal angle  $\gamma$  is given by

$$P(\beta) = P(0) \exp(-\beta^2/2\Gamma^2)$$

where  $\Gamma$  is the standard deviation.

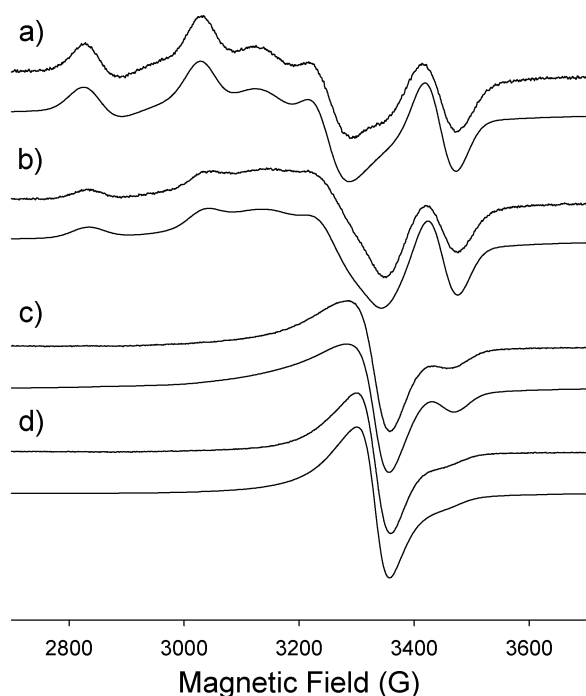


**Figure 7.** Experimental (top) and simulated (bottom) EPR spectra of  $[\text{Cu}(\text{cyclam})]^{2+}$ -saponite in oriented films for (a)  $\alpha = 0^\circ$ , (b)  $\alpha = 30^\circ$ , (c)  $\alpha = 60^\circ$ , and (d)  $\alpha = 90^\circ$ . The spectra were measured at room temperature.

First, we assume that the  $\text{CuN}_4$  plane is parallel to the clay layers, and thus the  $g_{\parallel}$  direction is parallel to the  $c$  axis. Then, the angle  $\theta$  between the magnetic field and the  $g_{\parallel}$  direction is given by

$$\theta = \cos^{-1}(\sin \alpha \sin \beta \cos \gamma + \cos \alpha \cos \beta)$$

Spectra were simulated by combining single-crystal spectra for the ranges  $\beta = 0-90^\circ$  and  $\gamma = 0-180^\circ$ . All orientation-dependent spectra could be simulated satisfactorily using the same EPR parameters and  $\Gamma = 20^\circ$ ; see Figure 7 and Table 1.

We have also considered the possibility that the  $\text{CuN}_4$  plane is inclined to the clay layers. If the  $g_{\parallel}$  direction is tilted from the  $c$  axis, EPR spectra for different directions of  $g_{\parallel}$  around the  $c$  axis should also be combined. The orientation-dependent EPR spectra have been simulated for a tilt angle of  $9.8^\circ$  (see Discussion section). The best overall fit is obtained with  $\Gamma = 10^\circ$ , but simulated spectra deviate considerably from the measured spectra at some directions of the magnetic field. For example, the simulated spectrum for  $\alpha = 60^\circ$  shows some hyperfine features of component B at 3000–3200 G that are absent in the experimental spectrum (Figure 8). The best fit between the experimental and simulated spectra is obtained when the  $\text{CuN}_4$  plane is assumed to be parallel to the clay layers.

## Discussion

**Components of EPR Spectra.** EPR spectra of  $[\text{Cu}(\text{cyclam})]^{2+}$ -saponite reveal two components with an intensity ratio of 6.5:1.0. The major component (component A) has the Lorentzian line shape and no hyperfine structure, indicating that it originates from molecules exchange coupled with adjacent molecules in the interlayers of saponite.<sup>14</sup>

The EPR parameters of component B are similar to those ( $g_{\parallel} = 2.174$ ,  $g_{\perp} = 2.038$ ,  $A_{\parallel} = 0.0213 \text{ cm}^{-1}$ , and  $A_{\perp} = 0.0029 \text{ cm}^{-1}$ ) of a frozen solution spectrum of  $[\text{Cu}(\text{cyclam})](\text{ClO}_4)_2$ .<sup>10</sup> The line shape of individual hyperfine line of  $[\text{Cu}(\text{cyclam})]^{2+}$ ,

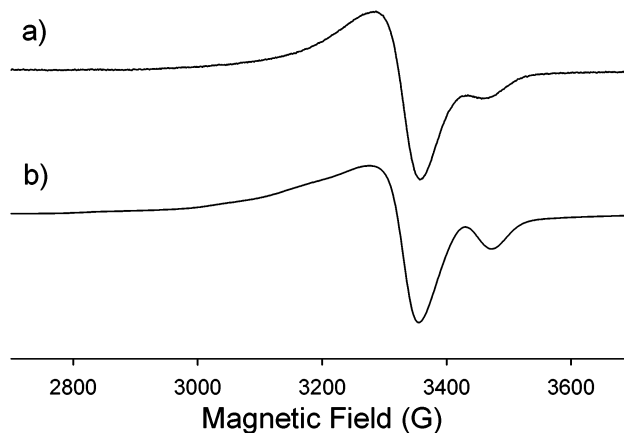


**Figure 8.** (a) Experimental and (b) simulated EPR spectra for  $\alpha = 60^\circ$ . The  $\text{CuN}_4$  plane is assumed to be tilted  $9.8^\circ$  from the clay layers.

which is determined mainly by unresolved superhyperfine lines due to the four nitrogen ligand atoms, is close to the Gaussian line shape.<sup>10</sup> So both the EPR parameters and the line shape agree with those of a dilute species free from exchange coupling.

The number of  $[\text{Cu}(\text{cyclam})]^{2+}$  per unit cell of saponite is 0.28 in our sample. If the  $\text{CuN}_4$  plane is parallel to the clay layers, the van der Waals width of  $[\text{Cu}(\text{cyclam})]^{2+}$  is estimated to be  $9.8 \text{ \AA} \times 10.6 \text{ \AA}$  from the molecular structure.<sup>7</sup> Since the surface area of one face of the unit cell is  $50 \text{ \AA}^2$  ( $5.44 \times 9.19 \text{ \AA}^2$ ),<sup>6</sup> there is one intercalated molecule per 3.6 unit cells covering the faces of two of them. Therefore, many molecules can have adjacent molecules in the interlayers of saponite. If the adjacent molecules lie side by side, the copper–copper distance is ca.  $10 \text{ \AA}$ . Although this copper–copper distance is quite large,<sup>15</sup> component A suggests that exchange interaction among copper atoms is still strong enough to collapse the hyperfine splitting. If the adjacent molecules are displaced by one unit cell, the copper–copper distance is ca.  $14 \text{ \AA}$ . Since exchange interaction diminishes rapidly as the metal–metal distance increases, it is probable that no significant exchange interaction occurs at this copper–copper distance.<sup>16,17</sup> Therefore component B may be attributed to the molecules having no adjacent molecules lying side by side.

If component B originates from the exchange-free species in the clay interlayers, the ratio of components A and B should be sensitive to the number of  $[\text{Cu}(\text{cyclam})]^{2+}$  per unit cell. To increase the relative amount of component B, we have prepared a sample in which the number of  $[\text{Cu}(\text{cyclam})]^{2+}$  per unit cell of saponite is 0.08. If the intercalated  $[\text{Cu}(\text{cyclam})]^{2+}$  species were evenly distributed in the interlayers, most of the copper species should be exchange free. But the EPR spectrum shows that the ratio of components A and B does not decrease as expected, indicating that there is a highly loaded domain. Irregular domain formation has been suggested for other clays at low CEC loadings.<sup>18</sup> More work is needed to determine the relation between the concentration of  $[\text{Cu}(\text{cyclam})]^{2+}$  in the clay and the ratio of components A and B.

The  $g$  value (2.046) of component C for montmorillonite and hectorite is similar to that of the powder spectrum of pure  $[\text{Cu}(\text{cyclam})](\text{ClO}_4)_2$ . Each molecule is surrounded by six molecules at copper–copper distances of  $8.0\text{--}8.7 \text{ \AA}$  in the single crystal of  $[\text{Cu}(\text{cyclam})](\text{ClO}_4)_2$ ,<sup>7</sup> and the exchange interaction is strong enough to collapse the hyperfine splitting. Since three-dimensional aggregates of  $[\text{Cu}(\text{cyclam})]^{2+}$  cannot exist in the clay interlayers, component C is tentatively attributed to pure  $[\text{Cu}(\text{cyclam})](\text{ClO}_4)_2$  powder deposited on the surface of the clay platelets.



**Orientation of [Cu(cyclam)]<sup>2+</sup> in the Interlayers of Saponite.** Our spectra are best simulated when the CuN<sub>4</sub> plane is assumed to lie parallel to the clay layers. Then the height of the molecule seems to exceed the gallery spacing. The crystal structure of [Cu(cyclam)](ClO<sub>4</sub>)<sub>2</sub> shows that the copper atom lies at a crystallographic center of symmetry and the four nitrogen atoms form a square plane.<sup>7</sup> The six-membered chelate ring adopts a flattened chair conformation, and the maximum distance of displacement of a hydrogen atom (H<sub>12</sub> in ref 7) from the CuN<sub>4</sub> plane is 1.85 Å. So when the van der Waals radius<sup>19</sup> of the hydrogen atoms (1.20 Å) is added, the molecular size is estimated to be 10.6 × 9.8 × 6.1 Å<sup>3</sup>. The molecular height (6.1 Å) is much larger than the gallery spacing of 3.75 Å. But the gallery spacing, obtained by subtracting the thickness of the silicate layer (including the van der Waals radius of two oxygen atoms) from the basal spacing,<sup>20</sup> represents the minimum spacing between two oxygen atoms in the top and bottom surfaces of the interlayer. The spacing is much larger than 3.75 Å below or above the hexagonal cavities formed by oxygen atoms on the interlayer surfaces.<sup>21</sup> If some hydrogen atoms key into these cavities, the interlayer can accommodate a molecule whose height is larger than the gallery spacing. Keying of various intercalated molecules is well established for some other clay systems by IR, inelastic neutron scattering, and cross-polarization NMR studies.<sup>22–24</sup>

We drew contour maps of the top and bottom surfaces of the interlayer using the atomic coordinates<sup>20</sup> and the van der Waals radius of the oxygen atoms and tried to fit the [Cu(cyclam)]<sup>2+</sup> ion between the two surfaces. It turned out that the two axial hydrogen atoms of the six-membered ring, which have an interatomic distance of 2.55 Å, should key into the same hexagonal cavity on one surface. The two axial hydrogen atoms of the other six-membered ring key into the same hexagonal cavity on the other surface. Since the two hydrogen atoms can penetrate only partially into the same hexagonal cavity, the maximum molecular height that can be accommodated in the interlayer with a gallery spacing of 3.75 Å is estimated to be 5.3 Å, a value still considerably smaller than the molecular height.

The height of the “free” molecule can be reduced, if the confining interlayer region of clay forces the intercalated molecule into more planar arrangement.<sup>25</sup> Gallery spacings that are 4 Å smaller than the estimated molecular heights have been reported for hectorites intercalated with some Cu(II) phthalocyanines,<sup>25</sup> and both keying and flattening of the intercalated molecules should be responsible for the large difference between the gallery spacing and the molecular height. However, more sophisticated calculations such as molecular dynamics simulation are needed to determine whether the chair conformation of the six-membered rings of [Cu(cyclam)]<sup>2+</sup> can be so flattened in the clay interlayer that the height of the axial hydrogen atom decreases by 0.4 Å.

Since the two six-membered chelate rings lie above and below the CuN<sub>4</sub> plane, another way to reduce the molecular height is to tilt the CuN<sub>4</sub> plane relative to the clay layers. The minimum molecular height (5.2 Å) is obtained, if the CuN<sub>4</sub> plane is inclined to the clay layers by 9.8°. Although this molecular height can be accommodated readily in the interlayer without significant change on the molecular conformation, the simulated spectra for the inclined CuN<sub>4</sub> plane deviate considerably from the experimental spectra at some directions of the magnetic field (Figure 8).

**System with an Inclined Molecular Plane.** While considering the possibility that the CuN<sub>4</sub> plane of [Cu(cyclam)]<sup>2+</sup> is

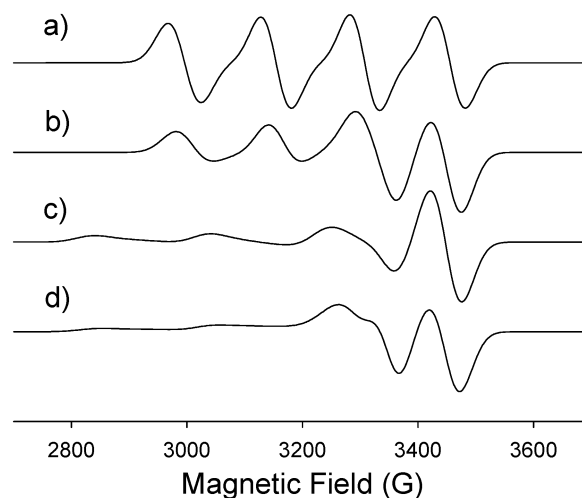


**Figure 9.** Simulated EPR spectra of CuTMPyP in fluorohectorite for (a)  $\alpha = 0^\circ$ ,  $\Gamma = 0^\circ$ , (b)  $\alpha = 90^\circ$ ,  $\Gamma = 0^\circ$ , (c)  $\alpha = 0^\circ$ ,  $\Gamma = 20^\circ$ , (d)  $\alpha = 90^\circ$ ,  $\Gamma = 20^\circ$ . The molecular plane was assumed to be inclined  $45^\circ$  to the clay layers.

inclined to the clay layers, we have found some apparent misunderstandings about EPR spectra of such systems in the literature.<sup>3,4</sup> The EPR spectra with the magnetic field parallel and perpendicular to the film surface look very similar for the Cu(II) tetrakis(*N*-methyl-4-pyridiniumyl)porphyrin (CuTMPyP) cation in fluorohectorite, and it has been suggested that the spectra should be the same, when the molecular plane is inclined to the clay layers by  $45^\circ$ .<sup>4</sup> But this cannot be generally true. Let us first assume that the *c* axes of all clay platelets are perpendicular to the glass surface. When the magnetic field is perpendicular to the glass surface, the angle  $\theta$  between the magnetic field and the *g*<sub>||</sub> direction is  $45^\circ$  for all molecules and a single-crystal-type spectrum should be observed (Figure 9a).<sup>26</sup> In contrast, when the magnetic field is parallel to the glass surface,  $\theta$  varies from  $45$  to  $90^\circ$  and a quite different spectrum should be observed (Figure 9b).

No hyperfine feature of  $\theta = 0^\circ$  is expected to be seen at these directions of the magnetic field, but the experimental spectra show such hyperfine features.<sup>4</sup> This indicates that there are some molecules having their *g*<sub>||</sub> axes parallel to the magnetic field because some clay platelets are inclined to the glass surface. When a Gaussian distribution with the standard deviation of  $20^\circ$  is introduced for the *c* axis, the simulated spectra with the magnetic field parallel and perpendicular to the film surface now show hyperfine features corresponding to  $\theta = 0^\circ$ . Moreover, the spectra look similar to each other because they approach the powder spectrum (parts c and d of Figure 9). The experimental spectra have an additional component having no hyperfine feature,<sup>4</sup> which may be attributed to molecules exchange coupled with adjacent molecules. When the molecules are inclined in the interlayers of clay, the copper–copper distance can be less than  $10 \text{ Å}$  and the exchange interaction between adjacent molecules may be strong enough to collapse the hyperfine splitting. If more orientation-dependent spectra are available, the tilt angle of the molecular plane for this system may be determined by simulation of the spectra.

**Distribution of Inclined Clay Platelets.** Simulation of the orientation-dependent spectra produces the standard deviation of the Gaussian distribution for the inclined clay platelets. Since this is a measure of the disorder in the alignment of the clay platelets, it may be called a disorder parameter. Parameter  $\Gamma = 0^\circ$  represents a perfect alignment of the clay platelets in the *z*

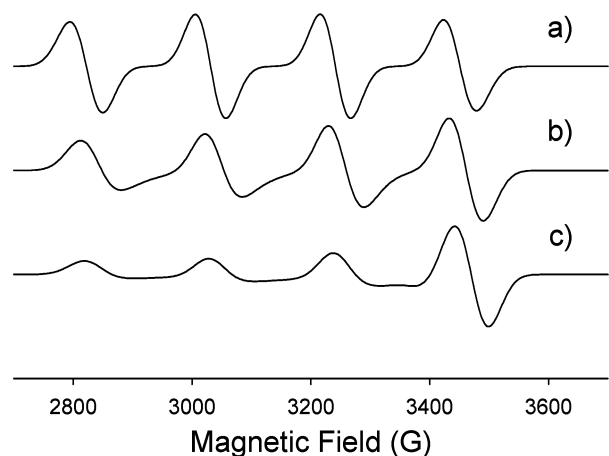


**Figure 10.** Simulated EPR spectra of CuTMPyP in hectorite for different standard deviations of the Gaussian distribution for the inclined clay platelets. (a)  $\Gamma = 0^\circ$  (perfect alignment), (b)  $\Gamma = 16^\circ$ , (c)  $\Gamma = 30^\circ$ . The magnetic field is perpendicular to the film surface.

direction. When  $\Gamma$  is greater than  $300^\circ$ , the spectrum looks very similar to the powder spectrum.

The orientation-dependent spectra are affected by both the distribution of inclined clay platelets and the orientation of the molecule to the clay layer, and both of them can be determined by simulating the spectra at various directions of the magnetic field. If the molecular orientation in the clay interlayer is known, the distribution of inclined clay platelets can be determined from the spectrum with the magnetic field perpendicular to the film surface alone. The EPR spectrum of CuTMPyP in hectorite shows four hyperfine lines when the magnetic field is perpendicular to the film surface.<sup>4</sup> But the spectrum is different from a single-crystal spectrum: the hyperfine line height increases with increasing magnetic field. This feature can be simulated by introducing a Gaussian distribution with a standard deviation ( $\Gamma$ ) of  $16^\circ$  (Figure 10b). This spectrum is compared with the calculated spectra with  $\Gamma = 0^\circ$  and  $\Gamma = 30^\circ$  in Figure 10. When clay platelets are perfectly aligned in the  $z$  direction, a single-crystal-type spectrum is obtained. Here, the two inner hyperfine lines look sharper than the outer lines, because the two isotopes of copper have slightly different hyperfine parameters. As  $\Gamma$  increases, the spectrum changes gradually to a powder type.

When clay films are prepared by casting, EPR spectra show that there is large disorder in the alignment of the clay platelets. The disorder parameter may be useful in developing methods to better align the platelets on a glass plate. To get a perfect platelet alignment in the  $z$  direction, we may use techniques recently developed for aligning zeolite microcrystals on glass plates.<sup>27</sup> These techniques attach "molecular glues" such as 3-chloropropyltrimethoxysilane to the surface of the glass plates and then chemically bond zeolite microcrystals to the glass surface.

We have shown that EPR spectra of partially oriented [Cu(cyclam)]<sup>2+</sup>-saponite platelets can be simulated. The result shows that there are two components in the spectra ascribable to exchange-narrowed species and exchange-free species, that the CuN<sub>4</sub> plane of [Cu(cyclam)]<sup>2+</sup> is parallel to the clay layers, and that the inclination of the saponite platelets to the glass surface can be described by a Gaussian distribution with a standard deviation of  $20^\circ$ . We have also shown that the EPR spectrum of the film with the magnetic field perpendicular to the film surface can be simulated using two different orientations of [Cu(cyclam)]<sup>2+</sup> to the clay layers. In previous EPR studies of oriented clay films by other authors, the partial orientation

of the clay platelets on the glass surface was neglected, and only the spectra with the magnetic fields perpendicular and parallel to the film surface were analyzed.<sup>2-5</sup> Our study shows that such analysis can produce an incorrect molecular orientation for a partially oriented system. Simulation of the EPR spectra with the magnetic field at various directions is needed to determine the correct molecular orientation.

**Acknowledgment.** We thank the U.S. NIH Research Resources program (RR-01811, R.L.B.) and University of Illinois research grants for facilities and support. H.S. thanks Sogang University for University Research Grant (2004). J.-H.C. thanks the Korean Ministry of Science and Technology for financial support through the National Research Laboratory Project '99.

## References and Notes

- (1) So, H.; Ha, K.; Lee, Y.-J.; Yoon, K. B.; Belford, R. L. *J. Phys. Chem. B* **2003**, *107*, 8281.
- (2) Clementz, D. M.; Pinnavaia, T. J.; Mortland, M. M. *J. Phys. Chem.* **1973**, *77*, 196.
- (3) McBride, M. B.; Pinnavaia, T. J.; Mortland, M. M. *J. Phys. Chem.* **1975**, *79*, 2430.
- (4) Giannelis, E. P. *Chem. Mater.* **1990**, *2*, 627.
- (5) Ukrainczyk, L.; Chibwe, M.; Pinnavaia, T. J.; Boyd, S. A. *J. Phys. Chem.* **1994**, *98*, 2668.
- (6) Choy, J.-H.; Yoon, J.-B.; Jung, H. *J. Phys. Chem. B* **2002**, *106*, 11120.
- (7) Tasker, P. A.; Sklar, L. *J. Cryst. Mol. Struct.* **1975**, *5*, 329.
- (8) Addison, A. W.; Sinn, E. *Inorg. Chem.* **1983**, *22*, 1225.
- (9) Miyoshi, K.; Tanaka, H.; Kimura, E.; Tsuboyama, S.; Murata, S.; Shimizu, H.; Ishizu, K. *Inorg. Chim. Acta* **1983**, *78*, 23.
- (10) Maimon, E.; Zilbermann, I.; Golub, G.; Ellern, A.; Shames, A. I.; Cohen, H.; Meyerstein, D. *Inorg. Chim. Acta* **2001**, *324*, 65.
- (11) Choy, J.-H.; Kim, D.-K.; Park, J.-C.; Choi, S.-N.; Kim, Y.-J. *Inorg. Chem.* **1997**, *36*, 189.
- (12) Choy, J.-H.; Kim, B.-W.; Park, J.-C.; Yoon, J.-B. *Mol. Cryst. Liq. Cryst.* **1998**, *311*, 303.
- (13) For some systems,  $w = w_{\parallel} \cos^2 \theta + w_{\perp} \sin^2 \theta$  gives better fit. See Hoffmann, S. K.; Zimpel, Z.; Augustyniak, M.; Hlilzer, W. *J. Magn. Reson.* **1992**, *98*, 1.
- (14) Anderson, P. W.; Weiss, P. R. *Rev. Mod. Phys.* **1953**, *25*, 269.
- (15) Broad hyperfine lines were observed from single crystals having a copper-copper distance of 6.8 Å and a vanadium-vanadium distance of 10.5 Å. See So, H.; Haight, G. P.; Belford, R. L. *J. Phys. Chem.* **1980**, *84*, 1849 and Téze, A.; Marchal-Roch, C.; So, H.; Fourier, M.; Hervé, G. *Solid State Sciences* **2001**, *3*, 329.
- (16) Kivelson, D. J. *J. Chem. Phys.* **1960**, *33*, 1094.
- (17) There is virtually no exchange narrowing for the Cu(II) or Co(II) tetrakis(*N*-methyl-4-pyridiniumyl)porphyrin cation intercalated parallel to the clay layers, where the metal-metal distance is 17 Å. See refs 4 and 5.
- (18) McBride, M. B. *Clays Clay Miner.* **1979**, *27*, 97.
- (19) Huheey, J. E.; Keitler, E. A.; Keitler, R. L. *Inorganic Chemistry*, 4th ed.; HarperCollins: New York, 1993; p 292.
- (20) The thickness of the silicate layer excluding the van der Waals radius of the oxygen atoms (1.50 Å) is 6.64 Å. For atomic coordinates of a smectite, see Viani, A.; Gualtieri, A. F.; Artioli, G. *Am. Mineral.* **2002**, *87*, 966. When the van der Waals radius of two oxygen atoms is added, the layer thickness becomes 9.6 Å. The gallery spacing (3.75 Å) was obtained by subtracting this value from the basal spacing of 13.35 Å.
- (21) For a good drawing of the hexagonal cavities, see Gaudel-Siri, A.; Brocorens, P.; Siri, D.; Gardebien, F.; Brédas, J.-L.; Lazzaroni, R. *Langmuir* **2003**, *19*, 8287.
- (22) Johnston, C. T.; Bish, D. L.; Eckert, J.; Brown, L. A. *J. Phys. Chem. B* **2000**, *104*, 8080.
- (23) Hayashi, S. *J. Phys. Chem.* **1995**, *99*, 7120.
- (24) Vahedi-Faridi, A.; Guggenheim, S. *Clays Clay Miner.* **1997**, *45*, 859.
- (25) Carrado, K. A.; Forman, J. E.; Botto, R. E.; Winans, R. E. *Chem. Mater.* **1993**, *5*, 472.
- (26) EPR parameters for Cu(II) tetrakis(*N*-methyl-4-pyridiniumyl)-porphyrin (Greiner, S. P.; Rowlands, D. L.; Krellick *J. Phys. Chem.* **1992**, *96*, 9132) were used for simulation to compare with the spectrum in ref 4.
- (27) (a) Kulak, A.; Lee, Y.-J.; Park, Y. S.; Yoon, K. B. *Angew. Chem., Int. Ed.* **2000**, *39*, 950. (b) Choi, S. Y.; Lee, Y.-J.; Park, Y. S.; Ha, K.; Yoon, K. B. *J. Am. Chem. Soc.* **2000**, *122*, 5201. (c) Ha, K.; Lee, Y.-J.; Lee, H.-J.; Yoon, K. B. *Adv. Mater.* **2000**, *12*, 1114.